Capture cross sections for the near symmetric ^{124}Sn + ^{96}Zr reaction

A. M. Vinodkumar,* W. Loveland, and P. H. Sprunger
Department of Chemistry, Oregon State University, Corvallis, Oregon 97331, USA

D. Peterson
Physics Division, Argonne National Laboratory, Argonne, Illinois 60439, USA

J. F. Liang, D. Shapira, R. L. Varner, and C. J. Gross
Physics Division, Oak Ridge National Laboratory, Oak Ridge, Tennessee 37831, USA

J. J. Kolata
Department of Physics, University of Notre Dame, Notre Dame, Indiana 46556, USA
(Received 7 October 2006; published 19 December 2006)

Capture-fission cross sections were measured for the near symmetric reaction between the massive nuclei ^{124}Sn and ^{96}Zr for center of mass energies from 195 to 265 MeV. Coincident fission fragments were detected and separated from elastic and deep inelastic scattering products by angle/energy/mass conditions. The measured capture cross sections agree quite well with calculations using the dinuclear system (DNS) model. The DNS model also predicts the fusion cross section for this reaction with a fusion barrier height of 208.0 MeV. The deduced extra push energy, corresponding to this barrier height, differs from that deduced from evaporation residue measurements.

DOI: 10.1103/PhysRevC.74.064612 PACS number(s): 25.70.Jj, 25.85.−w, 25.60.Pj

I. INTRODUCTION

The fusion of heavy symmetric and near symmetric nuclei exhibits an "extra push" effect. Evaporation residue (ER) cross section measurements [1–10] with massive projectiles ($A \sim 100$) have shown evidence for fusion hindrance with an extra energy being required to fuse the nuclei. The extra push model proposed by Swiatecki and Bjornholm [11,12], was successful in reproducing the experimental results.

The use of neutron-rich projectiles is thought to enhance fusion because of the lowering of the fusion barrier for the neutron-rich projectiles. However, studies done by Sahm *et al.* [1,2] for $^{90-96}$Zr + ^{124}Sn reactions suggested a canceling effect. It was shown that as the fusing system became more neutron rich (decreasing fissility, x) the fusion hindrance, measured by the extra push energy needed to get the nuclei to fuse, increased in contradiction to most theoretical models (see Fig. 1). If this were a general trend, the advantage of using radioactive beams in synthesizing new heavy n-rich nuclei would be significantly diminished.

We have performed an experiment at the Oak Ridge National Laboratory (ORNL) to measure the capture- fission cross sections for radioactive ^{132}Sn interacting with ^{96}Zr to investigate the isospin dependence of fusion hindrance. Because of the importance of the ^{124}Sn + ^{96}Zr system in understanding the ^{132}Sn + ^{96}Zr reaction, we have also measured the capture-fission cross section for the stable ^{124}Sn + ^{96}Zr reaction for near barrier energies. We report the results of that stable beam measurement in this article.

In Ref. [2], the capture and fusion cross sections were not directly measured but were deduced from measured evaporation residue cross sections. Ideally one would like to measure the fusion cross section directly. However, in systems like the ^{124}Sn + ^{96}Zr reaction, the separation of fusion events from other reaction processes, such as quasifission, is an experimental challenge. In this work, we use the capture-fission excitation functions to gain insight into isospin effects on entrance channel dynamics.

There have been many attempts to explain the evaporation residue cross section for massive nuclei using the dinuclear system (DNS) model [13–17]. The capture-fission cross section measurement described herein is complementary to an evaporation residue measurement. Reaction-specific or nuclei-specific effects in the fusion cross section should manifest themselves in the capture cross section. Fazio *et al.* [13] have investigated the entrance channel dependence of the fusion/capture of mass asymmetric or near symmetric systems using the DNS model in detail. Because this model is successful in reproducing the observed evaporation residue cross section, one can extract the fusion and capture cross sections from this model to compare with the measurements reported in this article.

The effect of entrance channel mass asymmetry in fusion was investigated by Hinde, Dasgupta, and Mukherjee [18] for the formation of ^{220}Th by comparing the evaporation residue cross section in the reactions ^{16}O + ^{204}Pb, ^{40}Ar + ^{180}Hf, ^{48}Ca + ^{172}Yb, ^{82}Se + ^{138}Ba, and ^{124}Sn + ^{96}Zr. They concluded that fusion is inhibited increasingly for reactions more symmetric than ^{16}O + ^{204}Pb. It is interesting to compare the capture excitation functions for forming ^{220}Th to better understand the role of entrance mass asymmetry in the fusion process.

*Electronic address: attukalv@onid.orst.edu

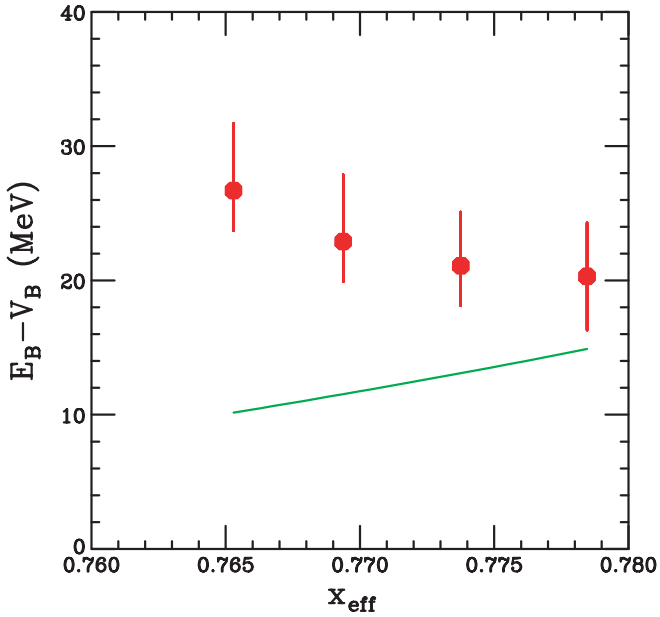

FIG. 1. (Color online) Extra push as determined from the mean fusion barrier height E_B and the barrier height calculated with the Bass potential, V_B, versus the effective entrance channel fissility x_{eff} [x_{eff} is defined as $x_{\text{eff}} = (Z^2/A)_{\text{eff}}/(Z^2/A)_{\text{crit}}$, where $(Z^2/A)_{\text{eff}} = 4Z_1Z_2/(A_1^{1/3}A_2^{1/3}(A_1^{1/3} + A_2^{1/3})$ and $(Z^2/A)_{\text{crit}} = 50.883(1 - 1.7826I^2)$ with $I = (N - Z)/A$]. The experimental points are taken from Refs. [1,2], with ^{124}Sn + ^{96,94,92,90}Zr systems selected. The theoretical prediction by Bjornholm and Swiatecki [12] is shown by a line.

In this article, we report the capture-fission cross section measurements for ^{124}Sn + ^{96}Zr for near Coulomb barrier energies.

II. EXPERIMENT

The experiment was performed at the Holifield Radioactive Ion Beam Facility (HRIBF) at ORNL [19]. ^{124}Sn beams with energies of 400–600 MeV were passed through a set of two microchannel plate detectors (MCPs) [20] separated by about one meter (that provided timing information) before striking an enriched ^{96}Zr (85.25%) target having a thickness of 380 μg/cm^2 in an evacuated scattering chamber. The ^{124}Sn beam intensity was $\sim 6 \times 10^5$ pps. Coincident reaction products were detected to measure fission. The experiment was carried out using two different setups. The schematic drawing of the two setups is shown in Fig. 2. In the first method, four double-sided silicon strip detectors (DSSDs) of thickness 300–500 μm were used for the detection of fission fragments. These detectors had an area of 5×5 cm^2 and provided energy, position, and time information for the detected fragments. These four silicon detectors were placed at a distance of 12.64 cm from the target covering an angular range of 20°–40° on either side of the beam. The detectors were calibrated using a ^{252}Cf source. The time of flight of the fragments striking the fission detectors was determined by the time difference between the signal from the Si detector(s) and a timing signal

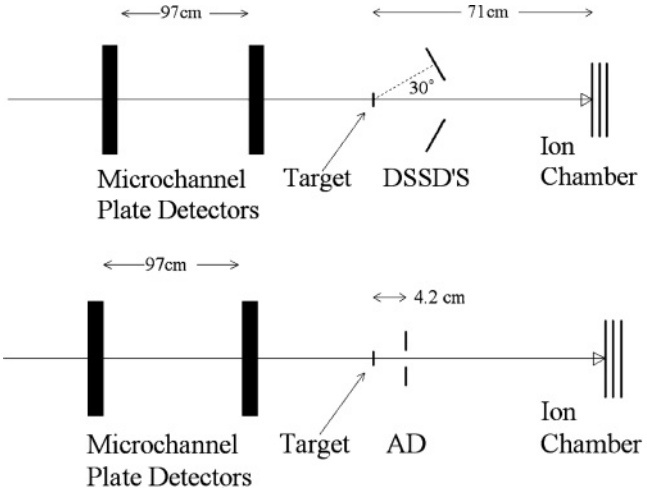

FIG. 2. The schematic drawing of the experimental setup. Four strip detectors (DSSDs) were used in the first setup, above and below the reaction plane, and in the second setup an annular detector (AD) was used.

from the second MCP. (MCP-MCP coincidences were used in tuning the beam to eliminate possible spurious events.) Elastic scattering with lower beam energies was used for time of flight calibration. The use of inverse kinematics focuses the reaction products forward, with the expected full momentum transfer fission fragments having a folding angle of ~70°–80°. A valid fission event is defined as a coincidence between two detected fragments with a folding angle corresponding to full momentum transfer. An ion chamber [21] was placed behind the scattering chamber to monitor the energy and number of beam particles.

In the second method, an annular silicon detector was used for the detection of fission fragments. In this case, the detector was placed at a distance of 2.9 or 4.2 cm away from the target at 0°. The annular segmented strip detector [22] had a thickness of 300 μm, an inner radius of 11.532 mm, an outer radius of 35 mm, and strip widths of 0.391 and 0.1 mm, respectively, for inner and outer strips. The first setup had an efficiency of 2% in detecting coincident fission events, and for the annular detector the efficiency was 7 and 14%, respectively, for the two detector positions used in the experiment.

The angles of the two coincident fragments (θ_1 and θ_2), their times of flight, and their respective energies (E_1 and E_2) allow a complete reconstruction of the binary process. The raw coincident experimental data can contain contributions from elastic scattering, inelastic scattering, and fusion-fission. To understand how these events can be separated, we show, in Fig. 3(a), a simulation of the expected coincident data for a pair of detectors at ±30° with respect to the beam and solid angles representative of the real detectors (±10°). Elastic scattering events are effectively cut out of the data by these angle cuts. Inelastic scattering events, such as the $Q = -40$ MeV events shown, can be detected but give energy (E) vs mass (M) correlations that are different from those of symmetric fission events. Gates can be set on the E vs M plots to isolate the symmetric fission events [Fig. 3(b)].

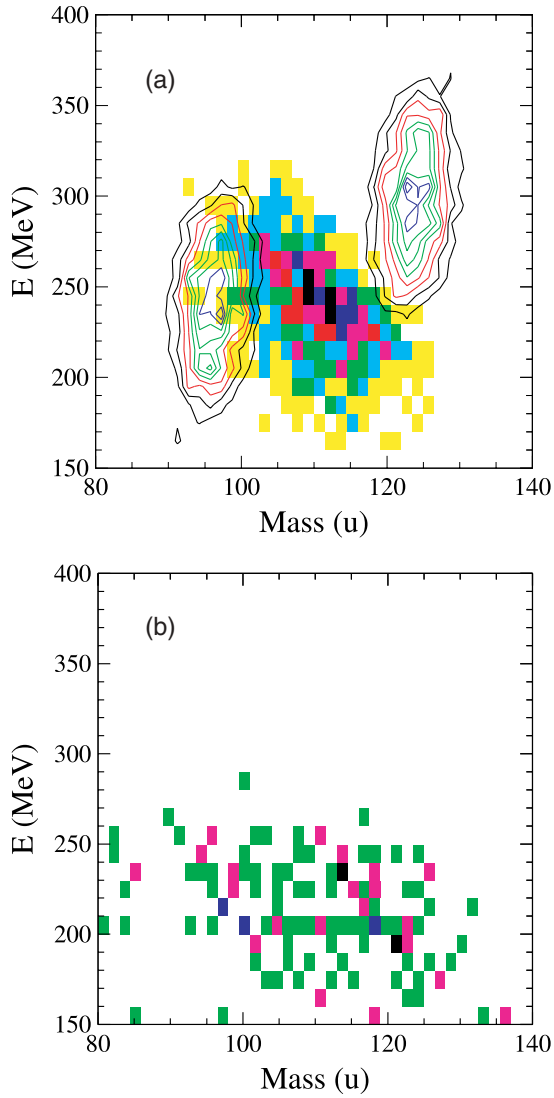

FIG. 3. (Color online) (a) Simulated coincident events for the reaction of 600 MeV ^{124}Sn with ^{96}Zr assuming the fragment detectors are at $30^\circ \pm 10^\circ$. The events arising from inelastic scattering with $Q = -40$ MeV are shown as contours while the symmetric fission events from the same simulation are shown in a scatter plot for ease of comparison with the experimental data in Panel (b). (b) The same plot as in Panel (a) except the points represent the measured data with gates applied to isolate the symmetric fission events.

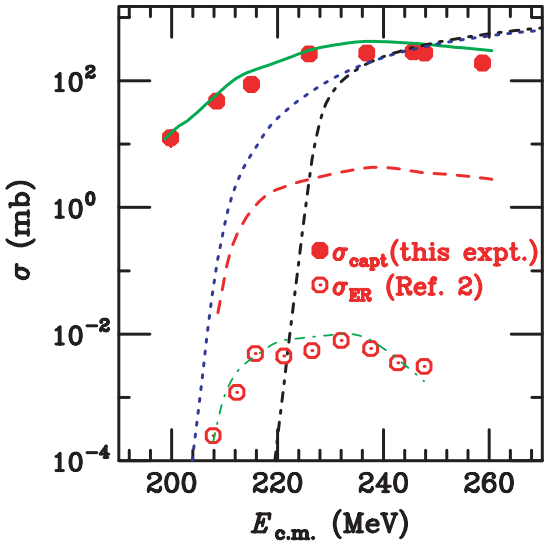

FIG. 4. (Color online) Excitation function for the ^{124}Sn + ^{96}Zr capture-fission reaction. The one-dimensional barrier penetration model prediction is represented by a thick dot-dashed line, the predicted capture and fusion cross sections using DNS model [30] are represented by solid and dashed lines, and the results of a coupled channels calculation are shown as a dotted line. The DNS model prediction for the evaporation residue cross section is shown as a thin dot-dashed line while the experimental data are from Ref. [2].

III. RESULTS AND DISCUSSIONS

The measured capture-fission excitation function is shown in Fig. 4, and the cross sections are listed in Table I. The thick dot-dashed line in Fig. 4 represents a one-dimensional barrier penetration model calculation having a barrier height of 227 MeV, a barrier radius $R_b = 12.0$ fm, and a barrier curvature $\hbar\omega = 4.2$ MeV obtained using a nuclear potential with $V_0 = 150$ MeV, $r_0 = 1.10$ fm, and $a = 0.63$ fm. In most of the heavy ion fusion reactions, enhanced cross sections with respect to a one-dimensional penetration model have been observed for below barrier energies. However, for above barrier energies, the one-dimensional penetration model usually gives reasonable agreement [23] with the data. In the case of ^{124}Sn + ^{96}Zr, the capture cross section is less than that predicted by the one-dimensional barrier penetration model for the above barrier energies, indicating a hindrance of the capture process and enhancement for the below barrier energies.

The results of a coupled channels calculation using the code CCFULL [24] are given by a dotted line in Fig. 4. The 2^+ and 3^- inelastic excitations of the target ($E_{2+} = 1.751$ MeV and $E_{3-} = 1.897$ MeV, deformation $\beta_2 = 0.08$, $\beta_3 = 0.27$ [25,26]) and projectile ($E_{2+} = 1.132$ MeV and $E_{3-} = 2.614$ MeV, deformation $\beta_2 = 0.122$, $\beta_3 = 0.1532$ [27,28]) were included in these calculations and no attempt was made to adjust the nuclear potential or diffuseness. These calculations are not able to reproduce the experimental data.

The production of evaporation residues is considered to be a three stage process in the DNS model. In the first phase, known as capture, nuclei overcome the Coulomb barrier and

TABLE I. The measured capture reaction cross sections for ^{124}Sn + ^{96}Zr. The c.m. beam energies are the energies calculated as corresponding to the center of the target beam energies. The errors are purely statistical.

$E_{c.m.}$ (MeV)	σ (mb)	$E_{c.m.}$ (MeV)	σ (mb)
199.8	13±3	208.5	48±7
215.1	88±5	226.0	265±20
236.9	275±19	245.6	288±11
247.8	275±17	258.7	191±12

form a molecule-like dinuclear system. In the second stage the transformation of the DNS into a more compact compound nucleus (CN) in competition with quasifission processes takes place. The cooling of the CN by emission of neutrons and charged particles constitutes the third stage of the DNS model. A detailed description of the model and discussion is given in Refs. [13,14,29]. It has been shown by Fazio *et al*. [13] that the DNS model calculations are able to reproduce the measured evaporation residue cross section for the ^{16}O + ^{204}Pb and ^{124}Sn + ^{96}Zr systems (Fig. 4). Using the same formalism with some improvements, Giardina, Mandaglio, and Nasirov [30] calculated the capture cross sections for the ^{124}Sn + ^{96}Zr reaction. The radius of each nucleus was calculated taking into account the distribution function of protons and neutrons. This method improves the calculations of the capture cross sections, particularly at lower energies compared to the result shown in Ref. [13]. These calculations are shown by a solid line in Fig. 4, which is in reasonable agreement with the experimental results, predicting a flattening or turnover in the capture cross sections at higher energies. These calculations suggest that competition between quasifission and fusion starts from low angular momentum values, with an increasing quasifission contribution to the reaction cross section as a function of increasing angular momentum. In the DNS model, the decrease of the cross section for energies $E_{\mathrm{c.m.}} \geqslant 240$ MeV is due to the "L-window effect"; i.e., at energies sufficiently above the Coulomb barrier, the capture of the projectile by the target nucleus becomes impossible because, after dissipation of a part of the relative kinetic energy, the system is not trapped into the potential at small values of the angular momentum. This effect is connected with the finite values of the friction forces calculated in the DNS model (see Fig. 1 of Ref. [14]). Quasifission is very significant in the case of reactions involving heavier nuclei.

The fusion cross section predicted by this model (given by the dashed line in Fig. 4) corresponds to a fusion barrier height of 208.0 MeV. This value is not in agreement with either the fusion barrier extracted from the evaporation residue cross sections (241^{+5}_{-3} MeV) in Ref. [2] nor the Bass model (214.3 MeV). Fusion barrier systematics have shown that the fusion barrier heights predicted by the Bass model exceed the measured barrier heights in the case of many heavy systems. Thus, our observations are not unexpected. However, in the case of the fusion barrier heights extracted for near symmetric heavy mass reactions in Ref. [2], they were substantially above the Bass model values.

The calculations [30] using the DNS model reproduce both the measured evaporation residue cross sections [2] and the measured capture cross section (this work) for the ^{124}Sn + ^{96}Zr reaction. Because of this "bracketing" of the physics involved by correctly describing the initial and final steps of the fusion-evaporation process, we give the greatest credence to the deduced fusion excitation function. This function shows no evidence for any significant extra push effect. Comparison of the predictions of the DNS model with results for the capture cross section for the ^{132}Sn + ^{96}Zr reaction (a measurement in progress) will clarify the role of isospin in fusion hindrance.

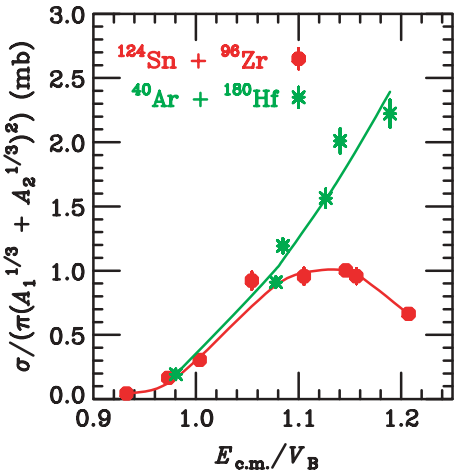

FIG. 5. (Color online) Reduced excitation function for the $^{124}_{50}$Sn + $^{96}_{40}$Zr and $^{40}_{18}$Ar + $^{180}_{72}$Hf reactions which both lead to ^{220}Th as a function of $E_{\mathrm{c.m.}}/V_B$. The ^{40}Ar + ^{180}Hf data were taken from Ref. [9].

In Fig. 5, the reduced capture cross sections are plotted against $E_{\mathrm{c.m.}}/V_B$, where V_B is the Bass model barrier height. The reduced cross section is obtained by dividing the cross section by $\pi(A_1^{1/3} + A_2^{1/3})^2$. This quantity, in the absence of fusion hindrance, should be $r_0{}^2$. The observed values of this quantity are substantially below what one expects for $r_0{}^2$, indicating significant fusion hindrance. At near barrier energies, both systems do not show any significant difference. However at higher energies (just 10 MeV above V_B), capture is suppressed in the case of ^{124}Sn + ^{96}Zr with respect to ^{40}Ar + ^{180}Hf. This suggests that fusion hindrance may start to take place at the contact configuration involved in the capture process.

IV. CONCLUSION

We measured the capture-fission cross section for the ^{124}Sn + ^{96}Zr system and compared it with different theoretical models. The DNS model gives a good representation of the data as well as previously measured evaporation residue cross sections. The deduced fusion barrier shows no anomalous hindrance effects.

ACKNOWLEDGMENTS

We thank Drs. Giardina, Mandaglio, and Nasirov for furnishing the results of their calculations prior to their publication. One of us (W.D.L.) thanks the Heavy Element Group at the Lawrence Berkeley National Laboratory for their hospitality during part of this work. This work was supported in part by the Director, Office of Energy Research, Division of Nuclear Physics of the Office of High Energy and Nuclear Physics of the U.S. Department of Energy under Grant DE-FG06-97ER41026 and Contract W31-109-ENG-38 and by the National Science Foundation under Grant PHY03-54828.

[1] C. C. Sahm *et al*., Z. Phys. A **319**, 113 (1984).
[2] C.-C. Sahm, H.-G. Clerc, K.-H. Schmidt, W. Reisdorf, P. Armbruster, F. P. Hessberger, J. G. Keller, G. Munzenberg, and D. Vermeulen, Nucl. Phys. **A441**, 316 (1985).
[3] A. B. Quint *et al*., Z. Phys. A **346**, 119 (1993).
[4] W. Reisdorf *et al*., Phys. Rev. Lett. **49**, 1811 (1982).
[5] W. Reisdorf *et al*., J. Phys. G: Nucl. Part. Phys. **20**, 1297 (1994).
[6] H. Ernst, W. Henning, C. N. Davids, W. S. Freeman, T. J. Humanic, F. W. Prosser, and R. A. Racca, Phys. Rev. C **29**, 464 (1984).
[7] K. T. Lesko, W. Henning, K. E. Rehm, G. Rosner, J. P. Schiffer, G. S. F. Stephans, B. Zeidman, and W. S. Freeman, Phys. Rev. C **34**, 2155 (1986).
[8] K.-H. Schmidt and W. Morawek, Rep. Prog. Phys. **54**, 949 (1991).
[9] H.-G. Clerc, J. G. Keller, C.-C. Sahm, K.-H. Schmidt, H. Schulte, and D. Vermeulen, Nucl. Phys. **A419**, 571 (1984).
[10] J. G. Keller, K.-H. Schmidt, H. Stelzer, W. Reisdorf, Y. K. Agarwal, F. P. Hessberger, G. Munzenberg, H.-G. Clerc, and C.-C. Sahm, Phys. Rev. C **29**, 1569 (1984).
[11] W. J. Swiatecki, Phys. Scripta **24**, 113 (1981); Nucl. Phys. **A376**, 275 (1982).
[12] S. Bjornholm and W. J. Swiatecki, Nucl. Phys. **A391**, 471 (1982).
[13] G. Fazio, G. Giardina, A. Lamberto, A. I. Muminov, A. K. Nasirov, F. Hanappe, and L. Stuttge, Eur. Phys. J. A **22**, 75 (2004).
[14] G. Fazio, G. Giardina *et al*., Phys. Rev. C **72**, 064614 (2005).
[15] A. Diaz-Torres, Phys. Rev. C **69**, 021603(R) (2004).
[16] G. G. Adamian, N. V. Antonenko, and W. Scheid, Nucl. Phys. **A678**, 24 (2000).
[17] G. Giardina, G. Fazio, F. Hanappe, G. Mandaglio, A. I, Muminov, A. K. Nasirov, and C. Sacca, Recent Res. Dev. Phys. **6**, 195 (2005).
[18] D. J. Hinde, M. Dasgupta, and A. Mukherjee, Phys. Rev. Lett. **89**, 282701 (2002).
[19] J. D. Garrett, Nucl. Phys. **A616**, 3c (1997).
[20] D. Shapira and T. A. Lewis, in *Proceedings of the 17th Conference on Application of Accelerators in Research and Industry,* edited by J. L. Duggan and I. L. Morgan (AIP CP680, 2003), p. 545.
[21] D. Shapira, J. F. Liang, C. J. Gross, R. L. Varner, H. Amro, C. Harlin, J. J. Kolata, and S. Novotny, Nucl. Instrum. Methods Phys. Res. A **551**, 330 (2005).
[22] Micron Semiconductor Ltd., Model No.S2.
[23] M. Dasgupta, N. Rowley, and A. M. Stefanini, Annu. Rev. Nucl. Part. Sci. **48**, 401 (1998).
[24] K. Hagino, N. Rowley, and A. T. Kruppa, Comput. Phys. Commun. **123**, 143 (1999).
[25] S. Raman, C. W. Nestor Jr., S. Kahane, and K. H. Blatt, At. Data Nucl. Data Tables **42**, 1 (1989).
[26] R. H. Spear, At. Data Nucl. Data Tables **42**, 55 (1989).
[27] J. Bryssinck *et al*., Phys. Rev. C **59**, 1930 (1999).
[28] J. Bryssinck *et al*., Phys. Rev. C **61**, 024309 (2000).
[29] G. Fazio *et al*., Mod. Phys. Lett. A **20**, 391 (2005).
[30] G. Giardina, G. Mandaglio, and A. K. Nasirov (private communication).